CHICAGO JOURNALS

vol. 181, no. 1 the american naturalist january 2013

E-Article

Linking Plant Disease Risk and Precipitation Drivers: A Dynamical Systems Framework

Sally Thompson,[1,*] Simon Levin,[2] and Ignacio Rodriguez-Iturbe[3]

1. Department of Civil and Environmental Engineering, University of California, Berkeley, California 94703; 2. Department of Ecology and Evolutionary Biology, Princeton University, Princeton, New Jersey 08544; 3. Department of Civil and Environmental Engineering, Princeton University, Princeton, New Jersey 08544

Submitted February 28, 2012; Accepted July 28, 2012; Electronically published November 27, 2012

Online enhancement: supplementary PDF.

abstract: Plant pathogens often respond sensitively to changes in their environmental conditions and consequently represent a potentially important ecological response to global change. Although several studies have considered the effects of increased temperature and CO_2 concentrations on plant pathogen risk, the effects of changing precipitation regimes have drawn less attention. Many classes of plant pathogen, however, are sensitive to changes in the water potential of their local environment. This study applied existing ecohydrological frameworks to connect precipitation, soil, and host properties with scenarios of pathogen risk, focusing on two water-sensitive pathogens: *Phytophthora cinnamomi* and *Botryosphaeria doithidea*. Simple models were developed to link the dynamics of these pathogens to water potentials. Model results demonstrated that the risk of host plants being colonized by the pathogens varied sensitively with soil and climate. The model was used to predict the distribution of *Phytophthora* in Western Australia and the severity of disease in horticultural blueberry trials with variable irrigation rates, illustrating potential applications of the framework. Extending the modeling framework to include spatial variation in hydrology, epidemic progression, and feedbacks between pathogens and soil moisture conditions may be needed to reproduce detailed spatial patterns of disease. At regional scales, the proposed modeling approach provides a tractable framework for coupling climatic drivers to ecosystem response while accounting for the probabilistic and variable nature of disease.

Keywords: ecohydrology, plant pathology, soil water potential, multiple stressors, dichotomous Markov noise, *Phytophthora cinnamomi*.

Introduction

Plant pathogens are important agents of disturbance, generating significant economic and environmental impacts in association with agricultural crop damage and plant mortality events. Plant pathogen epidemiology is often directly influenced by local edaphic and climatic factors (Agrios 2005) and may respond sensitively to relatively small changes in the local environment (Tapsoba and Wilson 1983; Maxwell et al. 1997; Mayek-Perez et al. 2002; Waugh et al. 2003; Thompson et al. 2010). The potential for altered pathogen ranges and epidemiology under future climates is considered to be a significant risk associated with global change (Coakley et al. 1999; Chakraborty et al. 2000; Boland et al. 2004; Garrett et al. 2006; Ibanez et al. 2006). Most studies examining the risks of altered pathogen behavior under future climate scenarios have focused on the role of temperature (Chakraborty 2005; Garrett et al. 2006; Thompson et al. 2010) and, in some cases, elevated atmospheric carbon dioxide concentrations (Pangga et al. 2004; Melloy et al. 2010) in altering pathogen dynamics. By contrast, there have been relatively few investigations of the potential for altered precipitation regimes to influence pathogen dynamics under future climate scenarios (Desprez-Loustau et al. 2006), despite the importance of water for the spread, survival, and disease potential of many plant pathogens.

Plant Pathogens in a Changing Rainfall Environment

An extensive body of research links water availability, and specifically ambient soil moisture or plant water potentials, to the dynamics of plant pathogens (Crist and Schoeneweiss 1975; Malajczuk and Theodorou 1979; Dickenson and Wheeler 1981; Madar et al. 1989; Boyer 1995; Schober and Zadocks 1999; Suleman et al. 2001; Desprez-Loustau et al. 2006; Ferrin and Stanghellini 2006). Many pathogens have a nonlinear response to changes in the hydration of their environment, which is manifest in terms of pathogen growth rates, survival, disease intensity, and reproductive behavior. The mechanisms that underlie this sensitivity may include changes in plant resistance to disease under waterlogged or drought conditions (Crist and Schoene-

* Corresponding author; e-mail: sally.thompson@berkeley.edu.

Am. Nat. 2013. Vol. 181, pp. E1–E16.
DOI: 10.1086/668572

weiss 1975; Madar et al. 1990; Boyer 1995) or changes in the behavior of pathogenic organisms themselves (Malajczuk and Theodorou 1979); no universal set of mechanisms has yet been defined (Desprez-Loustau et al. 2006). Schoeneweiss (1986) suggested a functional classification of pathogens on the basis of their sensitivity to water potential in their environment. Pathogens that were insensitive to water potential were regarded as "aggressive" (i.e., causing disease at all water potentials), those that responded linearly to altered water potential were classified as "intermediately aggressive" species, and "nonaggressive" species were those that caused disease only beyond a critical threshold in water potential. The aim of this study is to draw on the large body of ecohydrological theory that deals with the dynamics of soil moisture and plant water potentials to develop a simple theoretical framework to link precipitation, soil properties, and host species properties with disease risk. The focus is on "nonaggressive" species, in the sense of Schoeneweiss (1986), as these pathogens are most likely to display a sensitive response to altered climate or precipitation dynamics.

It is notoriously difficult to make generalizations about the epidemiology of plant pathogens, so the study focuses upon two relatively well-studied classes of pathogen with sensitivity to water potentials. The first are the *Phytophthora* water molds, and in particular *Phytophthora cinnamomi* (Pc). *Phytophthora* species are soil-borne pathogens that destroy plant fine root systems, starving plants of water and nutrients and ultimately causing death. As a contrasting example, stem canker pathogens, exemplified by *Botryosphaeria doithidea* (Bd) are considered. Canker-causing organisms enter host plants through wounds and then grow in the stem, colonizing the sapwood and ultimately girdling and killing their hosts. The main distinction between the pathogens here, however, is that Pc disease is promoted by wet conditions and inhibited in dry soils, while Bd mostly causes disease in drought-stressed plants. A brief review of the biology and water sensitivity of both species follows.

Biology of Phytophthora *Root-Rots*

Phytophthora cinnamomi is a mycelial oomycete (or "water mold"), which occurs either as a saprophyte or a root parasite infecting the fine roots of woody plants (Weste and Marks 1987; Harham 2005). Pc is highly destructive to susceptible plants, and is listed as a key threat to biodiversity in Australia (Environmental Protection and Biodiversity Conservation Act 1999). Pc is also associated with tree mortality and loss of commercial timber production in Hawaii, Europe, and North America (Newhook and Podger 1972; Hwang and Ko 1978; Balci and Halmschlager 2003; Judelson and Blanco 2005; Benson et al. 2006; Jönsson 2006). Pc is most problematic in wet soil conditions, which increase the growth of fungal mycelia, the rate of production, survival, motility of fungal propagules, and the infection potential of the pathogen (Hwang and Ko 1978; MacDonald and Duniway 1978; Nesbitt et al. 1978; Malajczuk and Theodorou 1979; Benjamin and Newhook 1981). By comparison, dry conditions can prevent or reverse Pc spread (Tippett et al. 1989). Pc is also sensitive to water potentials within host plants, with extension of fungal lesions and the progression of root mortality varying with water potential (Malajczuk and Theodorou 1979; Tippett et al. 1987). In sterile soil, water potentials exceeding −3,000 kPa are needed for pathogen growth (see fig. 1, supplemental material, available online), while disease symptoms within, for example, susceptible *Eucalyptus marginata*, are suppressed at phloem water potentials of less than −900 kPa (Tippett et al. 1987); these thresholds vary with soil type, fertility, and the host species (Sterne et al. 1977*a*,1977*b*). Pc cannot survive long periods of freezing temperatures (Bergot et al. 2004) and tends to be absent from rich soils with a diverse microflora community, apparently due to predation on the pathogen by amoebae and other soil organisms (Weste and Marks 1987). There is ongoing debate as to how Pc infection leads to plant mortality (Weste and Marks 1987; Davidson and Tay 1995; Maurel et al. 2001) and regarding the causes of the large variability in host susceptibility observed in many ecosystems (Weste and Marks 1987). The framework here will not explicitly address temperature variation or soil fertility and assumes that water stress is the dominant factor leading to mortality of hosts infected with Pc. It provides a tool for linking Pc dynamics to ecohydrologic variation but is not a comprehensive framework for interrogating Pc disease risk.

Biology of Botryosphaeria *Stem Cankers*

Botryosphaeria dothidea is a fungal pathogen that generates canker diseases in woody stems. Bd spreads through the vascular tissues of infected plants, causing bleeding necrosis, blocking xylem pit membranes, increasing cavitation risk, disrupting water and photosynthate transfer through the stem, and reducing hydraulic conductance of the plant (Crist and Schoeneweiss 1975; Madar et al. 1990; Vannini and Valentini 1994). The prevalence and severity of Bd increases with drought stress in a wide range of species (Pusey 1989; Brooks and Ferrin 1994; Smith et al. 1994; Rayachhetry et al. 1996; Ma et al. 2001). The most detailed studies of Bd sensitivity to water potentials examined the disease behavior in white birch (Crist and Schoeneweiss 1975). Growth of Bd stem cankers in white birch was inhibited when water potentials in the trees were maintained at over −1200 kPa, while water-stressed plants

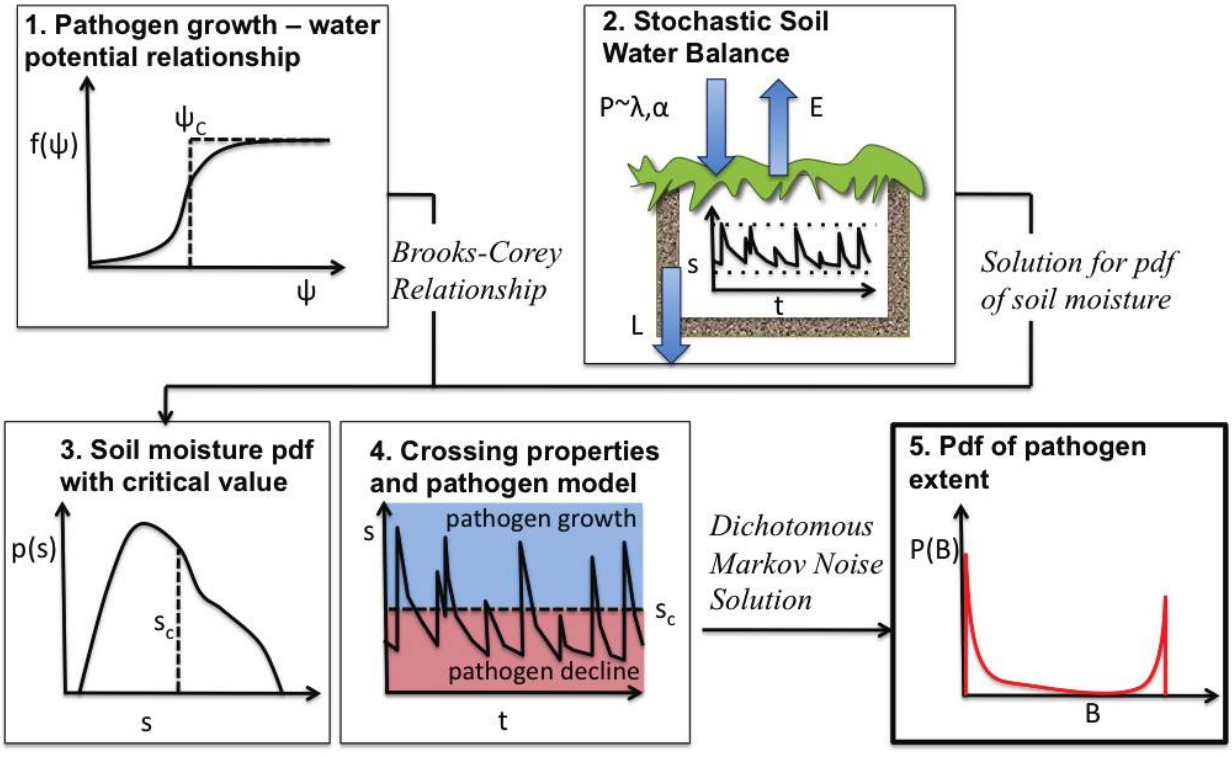

Figure 1: Diagram indicating the conceptual structure of the coupled soil moisture pathogen stochastic model developed here. Symbols: Ψ = water potential, Ψ_c = threshold water potential, P = precipitation, λ = precipitation frequency, α = mean storm depth, E = evaporation, L = drainage below the root zone, s = relative soil moisture, s_c = relative soil moisture at Ψ_c, t = time, B = pathogen extent.

with potentials of less than −1200 kPa developed disease symptoms. Removing water stress resulted in callus formation and decline of the pathogen, suggesting that the canker infections were reversible over some range of severity (Crist and Schoeneweiss 1975). The water potential sensitivity of Bd seems to be related to both a reduction in host resistance when stressed, as suggested by histological studies (McPartland and Schoeneweiss 1984), and to the intrinsic properties of Bd, as suggested by petri-dish studies (Ma et al. 2001). As with Pc, Bd epidemiology is not solely a function of drought stress in plants. Although Bd causes disease in water-stressed hosts, the pathogen requires wet conditions to spread (Ahimera et al. 2004), and the disease gains entry into plants through wounding (Rayachhetry et al. 1996; Rolshausen et al. 2010). Studies of Bd have not explored how extensive the canker can become before disease becomes irreversible. It is assumed here that Bd infection is present, if cryptic, in unstressed trees. Removal of water stress—if maintained indefinitely—is assumed to result in a complete recovery of the stem. These assumptions, although undoubtedly simplifications, provide a tractable starting point for developing a modeling framework.

Model Development

The model framework focuses on developing a simple model of pathogen dynamics and their effects on the stress experienced by the host plant and coupling it to existing ecohydrological models, as illustrated in figure 1. The pathogen growth rates are assumed to depend deterministically on the water potentials within the host plant, which can be directly related to soil water potentials (Ψ). Because these water potentials are driven by soil moisture availability, which fluctuates in time as a Markov process (Rodriguez-Iturbe et al. 1999), the pathogen growth rates themselves are stochastic. For both Pc and Bd, the dependence of the growth rates on the water potentials is similar to a step function, meaning that these fluctuations are dichotomous in nature: either the pathogen grows at its maximum rate, or the water availability is unfavorable and the pathogens grow at a minimum rate (which may be

zero). The critical water potential around which these fluctuations occur is termed Ψ_c. The probability density function (PDF) of processes forced by dichotomous Markov noise may be analytically determined using a solution presented by Horsthemke and Lefever (1984), provided that the statistics of the Markovian fluctuations (i.e., the soil moisture fluctuations) are known. To determine these statistics we draw on existing ecohydrological theories that predict the probability density function of soil moisture and its "crossing properties," that is, the frequencies of fluctuations in soil moisture around a given point. The existing theory allows the soil moisture PDF to be analytically predicted as a function of soil properties, rainfall statistics and evaporative demand. It therefore provides a mechanism to specify the fluctuations in the state of the pathogen purely as a function of (known) soil and climate properties. The role of existing theory in forging this link is shown conceptually in figure 1. Because this theory has already been extensively reported in the literature (Rodriguez-Iturbe et al. 1999; Laio et al. 2001) and is quite mathematically detailed, we do not reproduce it here.

Pathogen Model

To generate a simple model of Pc infection in a plant root system, several assumptions are adopted. Firstly, we assume that there is a maximum root volume v_{max} that can be sustained by the host tree. A completely healthy tree has a root volume v equal to v_{max}, with no infection in any of its roots. As Pc colonizes the host's root zone it impedes the function of and ultimately kills infected roots, so that the extent of the impeded roots, b, lies between 0 and v_{max}. In a host with resistance to Pc, new, uninfected roots regrow to replace dead or infected roots Newhook and Podger 1972; Weste and Taylor 1987. This has the effect of reducing the proportion of v_{max} impeded by Pc. The growth rate of Pc through the root volume reaches a maximum value in soils with water potentials greater than Ψ_c. In soils with water potentials below Ψ_c, the rate of root regeneration is assumed to exceed the rate at which infection expands, so that the infected root volume shrinks overall.

These assumptions are an approximation to the real dynamics of Pc infections and host recovery, the complete description of which requires a coupled model of both the pathogen growth and root turnover. With appropriate parameter choices, however, the Pc dynamics predicted by such a coupled model can be reasonably approximated by a single expression for b, based on the assumptions above. This point is justified in the supplemental material. The simplified expression takes the form

$$\begin{aligned} \frac{db}{dt} &= b(r(\Psi) - m) \qquad \text{for } b < v_{max}, \\ &= \min\,[b(r(\Psi) - m), 0] \quad \text{for } b = v_{max}, \end{aligned} \tag{1}$$

where

$$\begin{aligned} r(\Psi) &= r_{max} \quad \text{for } \Psi \geq \Psi_c, \\ &= r_{min} \quad \text{for } \Psi < \Psi_c. \end{aligned} \tag{2}$$

Here b [m^3] represents the volumetric extent of the host's root impairment due to both the spread of Pc and mortality of infected roots. Term b is bounded between 0 and the maximum rooting volume v_{max}. $r(\Psi)$ is the rate at which the pathogen extent increases throughout the host root system. Term m is the rate at which root regeneration reduces the proportion of the root system that is impaired by the pathogen activity. This rate is assumed to be constant regardless of host, soil water, or pathogen status, meaning that the total production of new roots is greatest when the pathogen has caused the most impairment. This approximation is most reasonable for woody species with large reserves of photosynthate that could be deployed to restore the root-shoot ratio. The growth rate of the fungal mycelia r (day^{-1}) is dependent on the plant water potentials, so that $r(\Psi) = r_{max}$ when $\Psi > \Psi_c$, and $r(\Psi) = r_{min}$ otherwise. That is, the growth response of Pc to water potential is approximated as a step function around a critical plant water potential value Ψ_c, a reasonable approximation to experimental observations (Malajczuk and Theodorou 1979) (see fig. 1 in supplemental material). Observations also indicate a reduction in Pc growth rates under permanently saturated conditions (Malajczuk and Theodorou 1979). Saturation rarely persists in most soils, so this reduction is neglected. As outlined in the supplemental material the plant water potential, soil water potential, and soil water content are readily interconvertible using the Brooks-Corey equation and an Ohm's law analogy for flow in the soil-plant system (Brooks and Corey 1964; Tyree and Ewers 1991).

The dynamics described by equation (1) are simple. Under wet soil conditions the pathogen spreads at its maximum rate r_{max}, colonizing the root zone. The extent of its proportional colonization is reduced by the production of new roots at rate m. If the soil becomes sufficiently dry, $r = r_{min} < m$, and the root zone of the hosts recovers. These linear dynamics prevail unless the extent of the pathogen infection increases so that $b \approx v_{max}$, in which case further growth of the pathogen does not result in further damage to the root zone of the host; that is, b is bounded by 0 and v_{max}.

The piecewise functional form in equation (1), while intuitive, makes further analysis awkward. A single-equation expression that maintains the $db/dt = 0$ condition at

$b = \nu_{max}$ can be formed by adjusting equation (1) with the nonlinear term $(b/\nu_{max})^n$:

$$\frac{db}{dt} = b(r(\Psi) - m) - \left(\frac{b}{\nu_{max}}\right)^n, \tag{3}$$

where, as $n \to \infty$, the steady state of equation (3), $b^* \to \nu_{max}$. The advantage of this nonlinear form is the rate at which the growth rate of the pathogen approaches zero as b approaches ν_{max} can be made arbitrarily fast by appropriate selection of n. The cutoff represents a maximum pathogen extent from the perspective of the infected plant (the pathogen cannot infect more than all of the plants roots) but not necessarily a point where pathogen growth should slow dramatically. In what follows $n = 100$, which causes the b growth dynamics to closely approximate a piecewise function of a constant growth rate for small b and a growth rate of 0 when $b \approx \nu_{max}$. In practice, a finite value of n results in the steady state value of b to be slightly less than ν_{max}. For $n = 100$, this steady state value deviates from ν_{max} by approximately 1%. This deviation can be made smaller by increasing n. Similarly, when $r = r_{min}$ and $b \approx \nu_{max}$ this formulation causes the rate of pathogen decline to be slightly overestimated while $(b/\nu_{max})^n$ is comparable in magnitude to $r_{min} - m$. This overestimation occurs only for b within 1% of the maximum value of ν_{max} and has no significant impact on the predicted dynamics. The simplicity of the expression in equation (3), however, is extremely valuable.

Equation (3) can be nondimensionalized by taking $B = b/\nu_{max}$, $t' = tm$, $R_{max} = r_{max}/m$ and $R_{min} = r_{min}/m$, so that

$$\begin{aligned} \frac{dB}{dt'} &= B(R(\Psi) - 1 - B^n), \\ R(\Psi) &= R_{max} \quad \text{for } \Psi > \Psi_c, \\ &= R_{min} \quad \text{for } \Psi \le \Psi_c. \end{aligned} \tag{4}$$

A very similar set of arguments can be made regarding stem canker dynamics, except that the canker growth is limited by the finite cross-sectional area of the stem and the soil moisture dynamics are imposed on the host resistance rather than the pathogen growth. The sensitivity of the growth rates to the water potentials is inverted for Bd compared to Pc, that is (again in nondimensional terms),

$$\begin{aligned} \frac{dC}{d\tau} &= C(1 - K(\Psi) - C^n), \\ K(\Psi) &= K_{max} \quad \text{for } \Psi > \Psi_c, \\ &= K_{min} \quad \text{for } \Psi \le \Psi_c, \end{aligned} \tag{5}$$

where K is a nondimensional mortality rate for the canker induced by host resistance, C is the canker areal extent nondimensionalized by the stem area A_s, and τ is time nondimensionalized against a fixed canker growth rate.

Dichotomous Markov Noise and the PDF of the Pathogen Extent

Having derived simple nondimensional expressions for the pathogen extent (eqq. [4], [5]), we can use the probabilistic dynamics of soil moisture and the theory of dichotomous Markov noise to derive an approximate probability density function for the pathogen extent. Equations (4) and (5) satisfy several criteria that are necessary to apply the solution methodology. First, the equations are stochastic ordinary differential equations multiplicatively driven by a Markovian random process (soil moisture variations; see Rodriguez-Iturbe et al. 1999; Rodriguez-Iturbe and Porporato 2004). Although the driving process can adopt many values, its effect on the pathogen dynamics is to introduce dichotomous switching around the soil moisture threshold (e.g., R and K adopt only two values). Secondly, a steady state condition exists for each of the two potential values of R and K. Finally, the steady state conditions differ for R_{min} and R_{max} and for K_{min} and K_{max} and bound the plausible range of values (0 to 1) of the state variables.

These conditions allow the analytical solution of Horsthemke and Lefever (1984) to be applied to determine the steady state PDF of the pathogen conditions B and C. This analytical solution for the PDF depends on the probability of switching around the soil moisture threshold and the form and parameters of equations (4) and (5). To apply the analytical solution, the governing equations are first reexpressed in terms of a stochastic "switch" Δ that can adopt values of 0 or 1, depending on the soil moisture. For the Pc case,

$$\begin{aligned} \frac{dB}{dt'} &= g(B) + h(B)\Delta, \\ g(B) &= (R_{min} - 1 - B^n)B, \\ h(B) &= (R_{max} - R_{min})B. \end{aligned} \tag{6}$$

That is, if $\Delta = 1$ the pathogen will grow, and if $\Delta = 0$ the host resistance will prevail. The Δ must be conditioned on the value of the plant water potential—or equivalently on the soil moisture—as follows:

$$\Delta(\Psi) = \begin{cases} \Delta_D = 0 & \text{for } \Psi \le \Psi_c \\ \Delta_W = 1 & \text{for } \Psi > \Psi_c \end{cases}. \tag{7}$$

Here the subscripts D and W refer to "dry" and "wet" conditions and are included for clarity. To compute the PDF of B, the derivations given in Muneepeerakul et al.

(2007) and Horsthemke and Lefever (1984) are followed. The switching behavior of Δ can be characterized by two frequencies, f^+ and f^-, which represent the frequency of switching across the soil moisture threshold from dry to wet (Δ_D to Δ_W) and from wet to dry (Δ_W to Δ_D). The probability associated with being in either of the moisture states can be expressed as

$$p(\Delta_W) = \frac{f^+}{\gamma^*}, \qquad p(\Delta_D) = \frac{f^-}{\gamma^*}, \tag{8}$$

where $\gamma^* = f^+ + f^-$. The mean value ($E(\Delta)$) of Δ is

$$E(\Delta) = \frac{1}{\gamma^*}(f^+ \times \Delta_W + f^- \times \Delta_D). \tag{9}$$

The connection to the soil moisture PDF and the rainfall statistics lies in f^+ and f^-. These values are determined from the "crossing properties" of the soil moisture. Term f^+, the frequency of crossing from below Ψ_c to above Ψ_c can be computed directly from the PDF of soil moisture ($p(\Psi)$) and the "loss function" (i.e., the sum of evaporation, deep drainage, and transpiration) for a given soil moisture $\rho(\Psi)$ (Porporato et al. 2001):

$$f^+ = p(\Psi_c)\rho(\Psi_c) \tag{10}$$

The computation of $p(\Psi_c)$ and $\rho(\Psi_c)$ as a function of the soil and climate properties is detailed in the supplemental material. Given f^+, the frequency of downcrossing can be computed from the probability p^+, where $p^+ = p(\Psi > \Psi_c)$. This is computed as $p^+ = 1 - \mathrm{CDF}(\Psi)$, where CDF indicates the cumulative distribution function of the soil moisture. Similarly, the probability of the water potential being less than the critical value is $p^- = \mathrm{CDF}(\Psi)$.

The steady state PDF of the variable B can be computed as

$$p(B) = N\frac{h(B)}{(g(B) + \Delta_W h(B))(g(B) + \Delta_D h(B))} \times \exp\left[-\gamma^* \int \frac{g(z) + E(\Delta)h(z)}{(g(z) + \Delta_W h(z))(g(z) + \Delta_D h(z))}\, dz\right]. \tag{11}$$

Substituting equations (7) and (9) into equation (11) and integrating, the PDF is obtained as

$$p(B_r) = -N'(R_{max} - R_{min})B^{a_1}(1 - R_{max} + B^n)^{a_2} \times (1 - R_{min} - B^n)^{a_3}, \tag{12}$$

where

$$a_1 = -\left(1 + \frac{f^+}{R_{min} - 1} + \frac{f^-}{R_{max} - 1}\right), \qquad a_2 = \frac{f^-}{n(R_{max} - 1)} - 1, \qquad a_3 = \frac{f^+}{n(R_{min} - 1)} - 1, \tag{13}$$

for $B \in [0, 1]$ and N' is a normalization constant chosen such that $\int_0^\infty p(B)dB = 1$.

Term B is defined on the region $B \in [0, 1]$. This analytical solution reproduces numerical simulations of the pathogen growth and plant recovery well, including the location of the mode(s) of the distributions at the extremes of $B = 0$ or $B = 1$ associated with the presence of the steady states (see fig. 2 in the supplemental material). The strength of the bimodality increases as f^+ and f^- decrease, meaning that the duration of excursions above or below s_c increases relative to the timescales of pathogen growth or loss. Less of the PDF mass is concentrated at the steady states as the f^+ and f^- increase, because soil moisture fluctuations tend to reverse net changes in pathogen biomass rapidly, providing a stabilizing influence. Eventually (with the appropriate parameter choice), the PDF collapses to a single mode.

The expectation of B can be computed analytically as

$$\overline{B} = \frac{1}{1 + a_1}(R_{max} - 2)^{-a_2}[(2 - R_{max})(R_{max} - 1)]^{a_2} \times (R_{max} - R_{min})(R_{min} - 2)^{-a_3} \times ((R_{min} - 2)(R_{min} - 1))^{a_3} \times A\left(\frac{1 + a_1}{n}; -a_2; -a_3; \frac{1 + a_1 + n}{n}; \frac{1}{R_{max} - 1}; \frac{1}{R_{min} - 1}\right), \tag{14}$$

where a_1, a_2, and a_3 adopt the values given in equation (13), and A is the Appell hypergeometric function of the first type (Appell 1925), defined as

$$A(\xi; \mu, \mu'; \eta; x, y) = \sum_{i=0}^{\infty}\sum_{j=0}^{\infty} \frac{\xi_{i+j}\mu_i\mu'_j}{i!j!\eta_{i+j}} x^i y^j. \tag{15}$$

The same derivation can be applied to the Bd canker dynamics described by equation (5). Since the host resistance rather than the growth rate is conditioned on the soil threshold for the Bd case, none of the other definitions of Δ or the probabilities need to be altered. The equations are

$$\frac{dC}{d\tau} = g(C) + h(C)\Delta, \text{ where} \qquad g(C) = (1 - K_{min} - C^n)C, \qquad h(C) = (K_{min} - K_{max})C, \tag{16}$$

with Δ defined as in equation (7) and C representing the dimensionless extent of the stem canker. Repeating the analysis in equations (8)–(11), the PDF for the stem canker disease is obtained as

$$p(C) = -N(K_{\max} - K_{\min})C^{a_1'} \times (C^n + K_{\max} - 1)^{a_2'}(C^n + K_{\min} - 1)^{a_3'}, \tag{17}$$

where

$$a_1' = \frac{f^+}{K_{\min} - 1} + \frac{f^-}{K_{\max} - 1} - 1,$$
$$a_2' = \frac{f^-}{n(1 - K_{\max})} - 1, \tag{18}$$
$$a_3' = \frac{f^+}{n(1 - K_{\min})} - 1,$$

and the expectation of the PDF is:

$$\overline{C} = -\frac{K_{\max}^{a_2'}[K_{\max}/(K_{\max} - 1)]^{a_2'}(K_{\max} - K_{\min})K_{\min}^{a_3'}[K_{\min}/(K_{\min} - 1)]^{-a_3'}}{2 + a_1'} \times A\left(\frac{2 + a_1'}{n}; -a_2'; -a_3'; \frac{2 + a_1' + n}{n}; \frac{1}{1 - K_{\max}}; \frac{1}{1 - K_{\min}}\right), \tag{19}$$

where A is again the Appell hypergeometric function (Appell 1925).

This analysis suggests that, at least for the case of pathogens whose growth dynamics depend simply on the ambient water potential, the steady state PDF of the pathogen condition can be estimated as a function of the rate parameters describing pathogen growth and host recovery, and the statistics of the fluctuations in soil moisture. The soil moisture fluctuations are directly dependent on soil properties, rainfall statistics, and evaporative demand (Rodriguez-Iturbe et al. 1999; Laio et al. 2001). Thus, this framework analytically links edaphic and climatic factors to likely pathogen responses.

Static Plant Stress

The model describing pathogen extent may be expanded to predict the physiological stress imposed by the pathogen on the plant. In this extension, the physiological stress is assumed to depend on the effects of pathogen tissue damage on water supply to the canopy. Other negative effects on the hosts such as toxin production or photosynthate consumption by the pathogen are not explicitly considered. Although the physiological effects on the host might be expected to scale linearly with the pathogen extent, in many cases the presence of the pathogen within a stem or root system may cause incomplete impairment of the function of the root systems or the stems. For instance, compensatory uptake by healthy roots may mean that infections of some proportion of the rooting volume contribute negligibly to the overall stress experienced by the host. Similarly, many plants can sustain high water fluxes through a relatively small proportion of their stem, as demonstrated by double saw-cut experiments (Schulte and Costa 2010). Consequently, a nonlinear relationship between physiological stress and the physical extent of a pathogen within a stem or root system is reasonable.

With these considerations, the concept of static—or instantaneous—stress experienced by a plant as described by Porporato et al. (2001) may be used to compute the stress induced in the plant by a pathogen with extent B (or C). There are two kinds of stress considered: (i) complete suppression of some proportion of the transpiration flux due to the effects of the pathogen (i.e., stress = 1), and (ii) a partial reduction of the remaining transpiration flux due to environmental water stress. The environmental water stress is computed using the approach of Porporato et al. (2001), in which stress is a nonlinear function of the water deficit: $[(s^* - s)/(s^* - s_w)]^{q_2}$. Here s is the relative soil water content, s^* is the satiation point at which plants experience no reduction in transpiration due to water scarcity, s_w is the wilting point at which water scarcity stops transpiration altogether, and q_2 parameterizes the nonlinearity in the plant's response to a given water deficit (Porporato et al. 2001). To compute a joint stress, these metrics are weighted by the proportion of the potential transpiration flux they affect. The reduction in the transpiration fluxes due to the pathogen is given by B^{q_1}. If $q_1 = 1$ then transpiration drops linearly with the pathogen extent, but if $q_1 > 1$ then the decline is nonlinear and may be trivial for small B. The environmental water stress is weighted by the unimpeded tissue's function $1 - B^{q_1}$, giving a joint stress:

$$\zeta(s) = B^{q_1} + (1 - B^{q_1})\left(\frac{s^* - s}{s^* - s_w}\right)^{q_2}. \tag{20}$$

The random variables B (e.g., normalized extension of the infection) and s (e.g., relative soil moisture) are assumed to be independent (see supplemental material for validation of this assumption). Given that B and s are independent, the expected value of the PDF of the joint water and pathogen stress may be computed from the PDFs of $[(s^* - s)/(s^* - s_w)]^{q_2}$ (given in Porporato et al. 2001) and the PDF of B computed above, as

$$\overline{\zeta(s)} = \overline{B}^{q_1} + \overline{(1 - B^{q_1})} \times \overline{\left(\frac{s^* - s}{s^* - s_w}\right)^{q_2}}. \tag{21}$$

Equation (21) quantifies the joint effect of pathogen and water stress in a mean-field sense.

Parameterization

Parameterization of the model requires estimates of pathogen growth rates during both expansion and reduction phases of growth. For Pc, the approach taken is to estimate a reasonable value for the maximum and minimum growth rates from laboratory data and then to treat the host resistance as a variable parameter. For Bd, the baseline growth rate, the "growth rate minus K_{min}" value is taken from greenhouse data, and the maximum host resistance K_{max} is treated as a variable.

The Pc growth rate data used are data describing mycelial extension obtained by Malajczuk and Theodorou (1979), who determined mycelial growth over a 10-day period from a fixed initial disk (assumed to have an initial length of 0.5 mm) introduced into 1.3-mm diameter tubing. Assuming uniform hyphal density and exponential growth, the maximum rate of mycelial growth was 0.46 day^{-1}. Under dry conditions, the minimum finite growth rate measured for Pc was 0.07 day^{-1}. Hosts with low resistance were assumed to impose a pathogen loss rate of 0.1 day^{-1}, and hosts with high resistance were assumed to impose a pathogen loss rate of 0.4 day^{-1}. These parameters exclude potential biochemical resistance in some plants, which may result in uniformly lower growth rates.

Bd growth rates in the absence of the host can be determined from experiments conducted by Ma et al. (2001) by fitting an exponential profile to colony diameter values obtained when growing Bd from 5-mm-diameter plugs on potato starch media. A growth rate of 2.4 day^{-1} was estimated from these data. Bd growth rates within plants can be obtained from Crist and Schoeneweiss (1975) in the same manner. The resulting value for the growth rate within the plant is 0.26 day^{-1}, suggesting that the minimum host resistance may be estimated as $\approx$ 2.1 day^{-1}. We assume that a slowly recovering host has a maximum resistance of 2.6 day^{-1}, while a rapidly recovering host has a maximum resistance of 3 day^{-1}. These data were used to develop the parameterizations in table 1.

Table 1: Parameterizations used in the models for *Phytophtora cinnamomi* (Pc) and *Botryosphaeria doithidea* (Bd) showing the growth and resistance parameters for the cases of a susceptible host (Growth max case for Pc and Resistance min case for Bd) and a resistant host (Growth min case for Pc and Resistance max case for Bd)

Resistance level	Growth max	Growth min	Resistance
Pc:			
Low	4.6	.7	1
High	1.15	.2	1
t'	10		
	Growth	Resistance max	Resistance min
Bd:			
Low	1	1.1	.875
High	1	1.25	.875
t'	.42		

Note: The values shown have been nondimensionalized as described in "Parameterization." Term t' shows the scaling factor for time, which is applied to the f^+ and f^- frequencies derived from the soil moisture dynamics in order to nondimensionalize the switching of the soil moisture around the critical value.

Model Implementation and Testing

The model was used to explore the sensitivity of the pathogen response and resulting host stress to climatic variations, soil texture, and depth. The model was then applied to three well-characterized case studies. Two relate to *Phytophthora cinnamomi* disease in Western Australia. The first case study explored the large-scale variations in Pc range (at scales of approximately 500 km × 500 km), while the second case study attempted to reproduce small-scale spatial variations in observed Pc disease in the forested Wungong water catchment (scales of approximately 5 km × 5 km). The third case study uses the model to estimate the relative severity of *Phytophthora cinnamomi* disease in terms of the root characteristics of infected Blueberry (*Vaccinium* sp.) under differing irrigation regimes.

Sensitivity Analysis. The model was initially applied for Pc and Bd to explore the mean pathogen extent and mean host stress for a range of reasonable rainfall statistics (mean storm depth $\alpha \in (0.1, 3)$ cm, and mean storm frequency $\lambda \in (0.01, 0.3)$ $days^{-1}$). The soil was assumed to be a loamy sand with a 30-cm rooting zone. Soil parameters were taken from the Clapp and Hornberger (1978) data set. The pathogen and host parameters used are given in table 1, and both the low and high resistance cases were simulated. The peak evapotranspiration was taken as 0.45 cm/day, and bare soil evaporation was assumed to be negligible. To explore the effects of soil texture and depth, these analyses were repeated for Pc using a fixed, intermediate rainfall case with $\alpha = 1.3$ cm and $\lambda = 0.3$ day^{-1}. The soil texture was varied through the five classes given by Clapp and Hornberger (1978): sand, sandy loam, loamy sand, sandy clay loam, and clay while maintaining the soil depth at 30 cm. The soil depth was then varied from 10- to 120-cm depth on a sandy loam. The resulting PDFs and means of Pc extent were recorded.

Case Study 1: Phytophthora cinnamomi *Range in Western Australia.* One advantage of the analytical framework is that it can be coupled to large-scale data sets of climate

and soils to make regional predictions. To illustrate the model's performance at these scales we used it to estimate the range of Pc in Western Australia. Pc was first known as "Jarrah dieback" disease in Western Australia in the 1920s (because Pc most obviously affected the timber species Jarrah, *Eucalyptus marginata*), and was positively identified as *Phytophthora cinnamomi* in 1965 (Weste and Marks 1987). Although there have been active quarantine efforts in Western Australia, this long disease history has allowed sufficient time for the disease to become established over a wide range in the southwest of the state. Southwest Western Australia is characterized by a strong decreasing rainfall gradient from coastal to inland areas, mirrored by a strongly increasing gradient in evaporative demand from the south coast into the interior. The southwest region has a diversity of soil types and depths. Native vegetation is highly susceptible to Pc disease, with the period of greatest disease risk occurring in the spring, when warming temperatures and moderate rainfall support Pc spread (Tregonning and Fagg 1984; Tippett et al. 1989).

Large-scale soil data for Western Australia are available from the Commonwealth Science and Industry Research Organization (2012) ASRIS data set, while the Australian Bureau of Meteorology provides gridded spatial mean monthly rainfall and mean monthly rain days data (Australian Government Bureau of Meteorology 2007, 2009). The rainfall data used were for the Australian spring period (defined as the months of September, October, and November). We note that although rainfall statistics can vary on a month-by-month basis, assuming fixed statistics on seasonal timescales produces a good approximation to the soil moisture PDFs (Rodriguez-Iturbe and Porporato 2004). The mean rainfall depth α (cm) was computed by dividing the cumulative mean spring rainfall for each pixel by the cumulative number of rain-days (the mean number of days with rainfall depths of greater than 1 mm recorded). The frequency of the rainfall events (λ day^{-1} was taken as the mean number of rain-days divided by the 90 days in the spring period. Mapped average areal evapotranspiration estimates (representative of the spring period) are available as image files (Australian Government Bureau of Meteorology 2005) and were manually digitized. Note that the Western Australian spring follows a cool, rainy winter. Winter rainfall statistics are similar to those in the spring, but evapotranspiration rates are lower. This may lead to an underestimation of the spring soil moisture and thus the pathogen risk during the seasonal transition.

Soil data are available to describe the clay content and soil depth of the A1, A2, B1, B2, and C horizons. The active soil layer was defined as the soils above the first occurrence of a heavy clay (% clay of $> 45\%$). The mean soil texture was estimated based on the depth-weighted average of the clay content in each layer. The mean percentage clay content was then used to classify the soils into the soil textural categories of Clapp and Hornberger (1978) to parameterize the soil moisture PDF model. The pathogen growth rates used correspond to the "susceptible" Pc case from table 1. For each approximately 7 × 7-km pixel, the expected value of the Pc severity, $\overline{B}$, was computed. We assumed that there would be a proportionality between $\overline{B}$ and the observation of population-scale disease at a site. Field and experimental trials indicate that established disease reduces the efficiency of the hydraulic apparatus (stomatal and stem conductances) of *Eucalyptus* species by 40%–60% (Dawson and Weste 1984; Crombie and Tippett 1990). This suggests that aboveground observation of disease symptoms might be most likely where $\overline{B} > \approx 0.5$. Accordingly we compared the model output to the mapped disease range of Pc. Maps indicating the contemporary range of Pc in Western Australia were obtained from the Center for *Phytophthora* Science and Management, and locations of Pc digitized for comparison with the model results.

Case Study 2: Phytophthora cinnamomi *Distribution in the Wungong Catchment.* At large scales, the model results reflect both soil and climatic variation. At small scales, climatic variation is relatively minor, and the roles of variable soil depth and texture should become more apparent. To explore the model performance at small scales, it was applied to a region of the Wungong Catchment (located approximately 62 km southeast of the city of Perth, Western Australia). Pc outbreaks in this catchment in the late 1960s were monitored using aerial photography and ground surveys (Batini and Hopkins 1972), allowing publication of a map depicting the presence of Pc disease in the Jarrah Forest over a 5 × 5-km area at a time when approximately 30% of the area was affected by visible Pc symptoms. This snapshot of the progressing Pc epidemic indicates highlights complex spatial patterns in disease emergence which appear to track soil type changes, stream courses, and roads. Climate data for the study region were taken from mapped rainfall averages for late spring, giving $\lambda = 0.15$, and a mean 8.5 cm of rainfall ($\alpha = 0.63$ cm). Potential evaporation was approximately 40 cm over the same period. Soil data were taken from the ASRIS data set and were processed in the same way as for the large-scale case to generate spatially variable maps of soil depth and textural properties. Again we assumed that the regions of disease establishment should approximately track regions in which likely disease severity was greatest.

Case Study 3: Phytophthora cinnamomi *Severity with Varying Irrigation in "Duke" Cultivars of Blueberry* Vaccinium *sp.* The previous case studies treat disease severity as a proxy for disease emergence at landscape scales. To address

disease severity directly we applied the model to a Pc outbreak associated with drip-irrigation of "Duke" cultivars of blueberry *Vaccinium* sp. reported by Bryla and Linderman (2007). Irrigation occurs three times a week at three rates, set to provide 50%, 100%, and 150% of the estimated transpiration demand (E_{max}, 358 mm over the 5-month growing season). Rainfall occurred additionally to the irrigation. To account for the combined effect of rainfall and irrigation water input, we forced the model with a value of λ that was derived from the sum of rainfall and irrigation water. In the absence of a time series of irrigation plus rainfall events, we estimated λ based on a synthetic time series of observed rainfall and regular irrigation using rainfall records from Corvallis, Oregon (Pacific Northwest Cooperative Agricultural Weather Network 2012). These data suggested that $\lambda_{rainfall}$ for the summer is around 1/13 days^{-1}, approximately a rain day every 2 weeks. The frequency of water input from the synthetic time series was $\approx$ 3.3/7 days. This value of λ, with α computed for the combined rainfall and infiltration volumes, was used for the simulation. The active soil depth was 0.3 m, set by the peak rooting depth observed in the study, in a loam soil. In horticultural settings, Pc disease often remains inactive at high water potentials—often as great as or exceeding field capacity (Sterne et al. 1977*a*, 1977*b*). We therefore chose to treat ψ_c as a calibration parameter. "Duke" cultivars are known to be susceptible to Pc (compared to other blueberry varietals), and therefore, the "susceptible host" growth parameters in table 1 were used. Mean soil moisture conditions were reported for the different irrigation rates (lumped across three irrigation types): drip irrigation consistently lead to a 3% higher volumetric water contents than the other irrigation methods used (sprinklers and microsprayers), and we adjusted the reported mean soil moisture accordingly. Root volume data were reported using a root vigor classification, ranging from 5 (where roots were large and vigorous, extending to a maximum root zone extent of 0.3 m) to 1 (roots that barely extended beyond the original root ball, estimated as approximately 5 gallons in volume based on standard pot sizes for the 2-year transplants, used to initiate the study). Normalizing the estimated root ball volume by the maximum volume, v/v_{max} ranged from 16% to 100%. This range was converted to pathogen extent B (by taking $B = 1 - v/v_{max}$) and then divided into four ranges: 0%–21% (vigor of 4–5); 21%–42% (vigor of 3–4); 42%–63% (vigor of 2–3); 63%–84% (vigor 1–2). The different irrigation rates lead to different root vigors: between 3 and 4 for the lowest irrigation rate, between 2 and 3 for irrigation at 100% of E_{max}, and between 1 and 2 for irrigation at 150% of E_{max}. We adjusted ψ_C so that the highest irrigation rate lead to $B \approx 70\%$, and computed the PDFs of soil moisture, the pathogen extent B, and the expected values of each of these distributions. We note that the authors also isolated *Pythium* species of root fungi from the blueberries; however, the relationship between *Pythium* and root vigor was not statistically significant, and *Pythium* was also found in individuals with otherwise intact root systems. The alterations in the root system extent are therefore attributed to the action of *Phytophthora*.

Results and Discussion

Sensitivity Analysis

The response of the pathogen extents and stress in the hosts is shown in figure 2 as a function of variable rainfall statistics. Sharp threshold transitions in pathogen risk and extent are obvious, lying along contours in the α, λ space. The contours of mean B and C risk approximately track contours of the mean rainfall rate (given by $\lambda\alpha$). This reflects that the timescales of disease development remain relatively long compared to the soil moisture fluctuations, allowing the pathogen response to integrate over the climatic variability. The host response mediated the transition between favorable and unfavorable conditions for Pc and Bd, with this transition being more abrupt for susceptible hosts. Altering host resistance had only a small impact on the predicted prevalence of stem canker disease but led to a large increase in the prevalence of Pc. This presumably reflects that very dry conditions were needed to completely inhibit Pc when $\Psi_c = -3{,}000$ kPa, so that host resistance played an important role across a wide range of climates. Climate was more generally limiting for Bd. When a combination of pathogen and drought stress was considered it was evident that Bd did not greatly exacerbate the static stress conditions experienced by its hosts: water stress was the dominant factor in determining the host stress. By contrast, drought and pathogen stress acted synergistically in the case of Pc and defined a restricted climatic space in which stress on the plants was minimized. The sensitivity of the pathogen extent to soil texture and soil depth were also explored with respect to Pc. Pc risk increased from $\overline{B} = 0.1$ to $\overline{B} = 0.7$ as soil texture was altered from sand to clay while holding rainfall constant ($\alpha = 1.3$ and $\lambda = 0.3$). Increasing soil depth (Z_r) tended to increase the Pc risk, but the relative increase in risk per increment in depth declined as the soil depths increased. For instance, doubling soil depth from 10 to 20 cm lead to a fivefold increase in the mean Pc extent (from $\overline{B} = 0.1$ to $\overline{B} = 0.5$). Doubling soil depth from 60 to 120 cm under the same conditions, however, caused only an ~8% increase in $\overline{B}$ (from $\overline{B} = 0.72$ to $\overline{B} = 0.78$). These dynamics were largely due to the likelihood of the shallow soils drying out between rainfall events, a dynamic that effectively prevents Pc establishment. The risk of drying

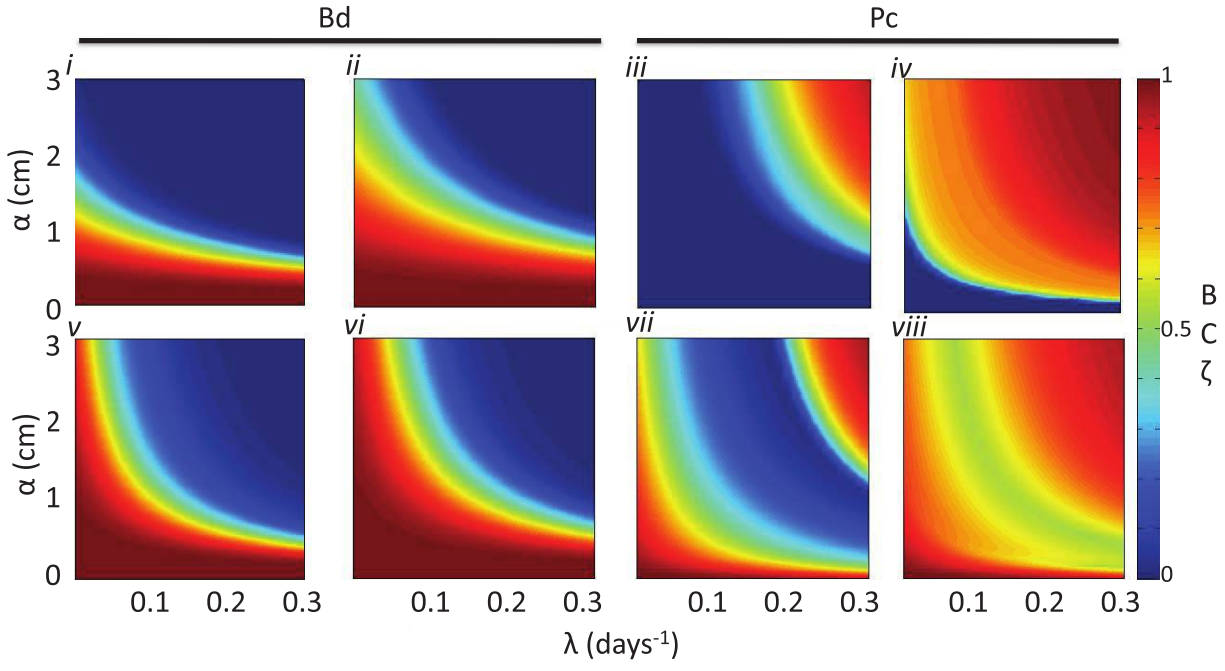

Figure 2: Expected values of the pathogen extent and the resulting plant stress for varying rainfall frequencies (λ day^{-1}) and mean depths (α cm), using the parameters given in table 1 assuming a 30-cm root zone in loamy sand soils and E_{max} is 0.45 cm. The top row shows the pathogen extents for *Botryosphaeria doithidea* (Bd) (*C*) in hosts with low susceptibility (*i*) and high susceptibility (*ii*), and *Phytophtora cinnamomi* (Pc) extents (*B*) in hosts with low and high susceptibility (*iii*, *iv*). The bottom row shows the corresponding host stress (ζ) for the pathogen behavior in the panel above it. The stress was assumed to be nonlinear in the pathogen extent, with $q_1 = q_2 = 3$. The color scales are identical for all panels.

out the soils declines rapidly as Z_r increases from 10 cm, but decreases only slightly with increasing Z_r for deep soils, so that Pc risk depends most sensitively on depth when Z_r is small.

Case Study 1: Phytophthora cinnamomi *Range in Western Australia*

A comparison between the predicted Pc severity and observations of Pc disease in the southwest of Western Australia is shown in figure 3. The results indicate that, in natural (susceptible) vegetation and subject to spring rainfall conditions, Pc would establish and persist in coastal regions throughout the southern and southwestern part of the state. This range declines sharply about 100 km inland and in the northern extent of the modeled range. The model predictions have an excellent correspondence with the reported current range of Pc in Western Australia. While soil properties cause minor differences in the predicted Pc severity at small scales, the large scale trends strongly reflect the gradients in rainfall and potential evapotranspiration in Western Australia. It is likely that this analysis has overstated the absolute value of the Pc risk in the interior of the state: changing vegetation type and lower winter minimum temperatures (which may prevent long-term establishment of Pc) have not been included in the model and would be likely to reduce Pc risks in these areas.

Case Study 2: Phytophthora cinnamomi *Distribution in the Wungong Catchment*

A comparison between the predicted Pc presence and observations of Pc disease in the Wungong catchment (centered on 32°24′50.37″S, 116°3′3.90″E) is shown in figure 4. Interpretation of these results needs to account for the fact that the data represent a snapshot of a dynamically progressing epidemic: thus the lack of observations of Pc even in high risk areas is likely to be associated with the migration of the disease front, rather than indicating a "failure" of the model. The spatial features shown in figure 4, however, can be interpreted with the assistance of the model.

During winter and early spring, the risk of Pc was uniformly high ($\overline{B} \to 1$) across the Wungong Catchment. However during the late spring period (when temperatures warm and Pc growth peaks), the predicted Pc severity was $\overline{B} \approx 0.8$ on deep clay loams ("high-risk areas"), and $\overline{B} \approx$

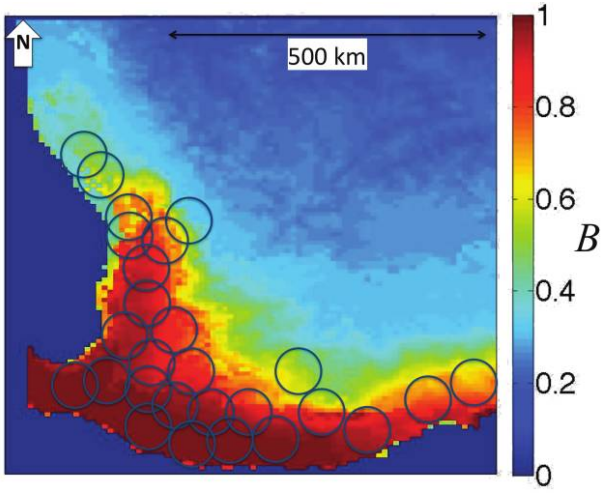

Figure 3: Predicted *Phytophtora cinnamomi* (Pc) extent (*B*) in Western Australia assuming sensitive vegetation and forcing the soil moisture model with spring rainfall and evapotranspiration. Circles indicate reported current range of Pc in Western Australia, as reported by the Centre for Phytophthora Science and Management, http://www.cpsm.murdoch.edu.au/.

0.4 on the shallower sandy loams ("low-risk areas"). When these soil regions were compared with the mapped disease extent, we found that Pc infection was observed on 28% of the low-risk area and on 53% of the high-risk area. That is, Pc occurred in low-risk regions at approximately half the rate at which it occurred in high-risk regions. This suggests that while Pc can become established in both soil types, there may have been an overall tendency for greater disease establishment in regions with finer-textured, deep soils. Appealingly, the proportionality in the rate of occurrence is comparable to the proportionality in $\overline{B}$ between the soil types. A strong association between Pc and the location of roads was visually evident when they are plotted together. However, proximity to roads alone did not explain any patterns in Pc risk through space (the Pc risk is approximately constant at around 40% at all distances from a road). However, when segregated by soil type, distance from a road affected Pc risk. In particular, the data show a large and monotonic decline in Pc risk on low-risk soils, from around 40% adjacent to roads to 10% at distances >200 m from roads. The elevation of Pc risk on low-risk soils near roads may reflect the significance of roads as dispersal corridors for disease and potentially the role of road drainage in locally elevating soil moisture conditions. The effect of the realistic increments of water that could be shed to the surrounding area was analyzed with a simple sensitivity analysis: a localized 10% increase in water availability (α) on low-risk soils increases the predicted Pc risk by 30%. A 50% increase in water availability on low-risk soils would result in the risk of Pc being equivalent to that of high-risk soils receiving only rainfall. The majority of Pc infection established in low-risk sites was associated with either proximity to Pc infection within a high-risk location or to a roadway, with the exception of the region labeled A (fig. 4). Location A is identified by Batini and Hopkins (1972) as a swampy region. We suspect that a perched water table (a hydrological elaboration not accounted for in the simple one-dimensional water balance used) may help provide locally suitable conditions for Pc at this location. Note also that the scale of soil mapping is coarser than the scale on which Pc outbreaks are mapped and that the location of transitions between soil types should therefore be interpreted with some caution. A final consideration is that some of the simplifying assumptions made in the model could result in a conservative prediction of disease occurrence. For instance, the probabilistic model assumes that there is no feedback between the pathogen condition and the soil moisture dynamics. Since Pc in particular directly affects the hydraulic system of the host plant, this assumption may be problematic in some cases (see supplemental material for a numerical investigation).

Phytophthora cinnamomi *Severity with Varying Irrigation in "Duke" Cultivars of Blueberry* Vaccinium *sp.*

The model output associated with this case study is shown in figure 5. Panel *A* shows the predicted PDF of soil moisture associated with the three irrigation regimes. The predicted PDFs of the pathogen extent are shown in panel *B*. A clear change in the pathogen behavior is evident between

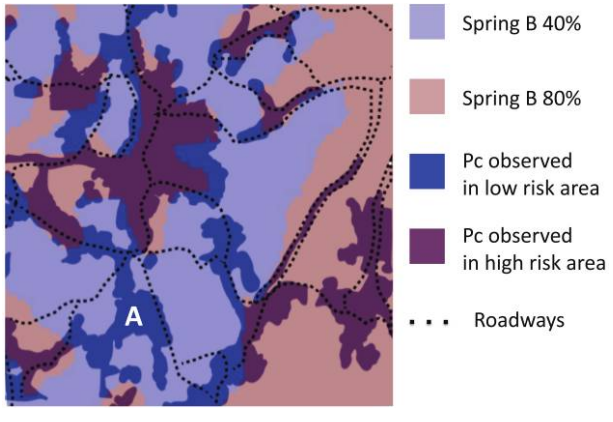

Figure 4: Comparison of *Phytophtora cinnamomi* (Pc) disease observed in the Wungong Catchment near Serpentine Dam, Western Australia, as reported by Batini and Hopkins (1972) with the predictions from the one-dimensional model.

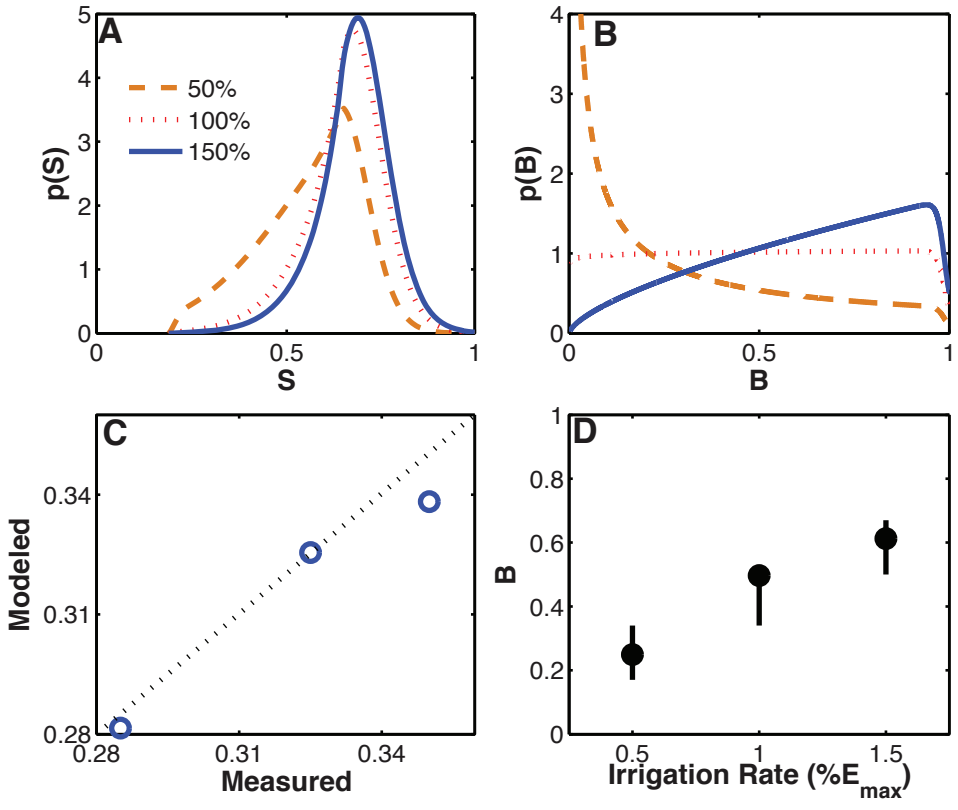

Figure 5: *A*, Predicted soil moisture probability density functions (PDFs) under the three irrigation regimes (50%, 100%, and 150% of E_{max}). *B*, Predicted PDFs of the pathogen damage to the root system for the three irrigation regimes. *C*, Comparison of the mean predicted soil moisture values with measurements; a dotted 1 : 1 line is included for comparison. *D*, Comparison of the predicted pathogen extent with the observations for each irrigation regime. Bars show the range of $\overline{B}$ associated with the root vigor estimates made for each irrigation regime.

the irrigation rate of 50% of E_{max} and the other irrigation rates. While the high frequency of water application ensured that soil could become wet enough to support Pc growth at the lowest irrigation rate, the relatively low volumes of applied water allowed the soil to dry out sufficiently between watering periods, inhibiting Pc growth. Panel *C* compares the expected value of soil moisture for each of the irrigation conditions against the measured mean soil moisture at the end of the growing season. Without any calibration the model correctly reproduced the mean soil moisture condition across the three treatments with a root mean squared error of 0.01. The deviations between model and measurement are comparable to typical measurement error in soil moisture calculations. Panel *D* shows the predicted mean pathogen extent predicted by the model for each irrigation treatment. The bars indicate the estimated range of the "vigor class" reported by Bryla and Linderman (2007) for each treatment. The results indicate that with minimal calibration the model can forecast soil moisture conditions and the resulting pathogen severity, given information about the cultural environment in which the crops were grown. Despite the limitations in the data, this case study demonstrates the ability of the modeling framework to (at least) semiquantitatively estimate the severity of pathogen infestation as a function of water input and edaphic conditions.

Conclusion

The potential for global change to exacerbate the economic, environmental, and social problems associated with plant pathogens is widely acknowledged (Coakley et al. 1999; Chakraborty et al. 2000; Boland et al. 2004; Garrett et al. 2006; Ibanez et al. 2006), as is the importance of resolving the major uncertainties associated with the feedbacks between climatic change and ecosystem changes (Lloyd and Farquhar 2008). Widespread outbreaks of plant disease are clearly one of the mechanisms (along with fire, herbivory, and drought; Allen et al. 2010) that have the potential to result in widespread, rapid, and potentially

irreversible changes to ecosystems. Developing frameworks that can relate climatic drivers to the risks of such mortality episodes remains an outstanding step in coupling these feedbacks to broader climate change predictions.

The framework presented here provides one approach to coupling physical and biological factors that relate to plant disease risk and impacts on individual trees. It addresses interactions of soil, water, evaporative demand, host, and pathogen properties to generate estimates of disease risk, assuming the pathogen is already present in the host system. Although the one-dimensional nature of the framework means it cannot be used to predict the spatial progression of disease, it appears to predict long-term pathogen ranges effectively based on rainfall, soil, and evaporation limitations alone. As such it is a useful complement to existing approaches that have primarily considered temperature as a control on pathogen ranges (Bergot et al. 2004). The framework appears capable of generating predictions of Pc severity as a function of cultural practices in managed conditions with minimal calibration. The model also proved useful as a tool to interpret high-resolution observations of spatial patterns of disease spread. Numerous avenues for future research were identified at these intermediate scales, however, including the value of linking models of pathogen spread to local edaphic conditions, potentially modeling such conditions using high-resolution distributed hydrological models to capture the complexities of water redistribution in sites with shallow water tables or significant riparian areas and the need to further explore the potential for dynamic feedbacks between pathogen impacts and biophysical conditions. Batini and Hopkins (1972), for instance, report that loss of canopy in diseased areas increased soil temperatures and accelerated rates of disease spread. They observed an approximately 10% increase in stream flow from the Wungong Catchment during the period of Pc spread, which they attributed to the disease. These findings, although anecdotal, illustrate the potential for disease to alter the energy and water balances of infected sites, leading to watershed-scale impacts. These feedbacks, and the implications of plant disease for ecosystem function as well as ecological change, remain open for exploration. They would form a particularly interesting comparison with similar natural disturbances that "turn off" canopy transpiration without disturbing soils (and are thus distinct from fire, landslide events, or clear cutting). Such disturbances include pine beetle outbreaks (Brooks et al. 2010) and climate-driven tree mortality events (Guardiola-Claramonte et al. 2011). These disturbances offer natural experiments with which to explore the dependence of landscape-scale biophysical processes on canopy transpiration and thus the potential land surface feedbacks of climatically induced herbivory, disease, or mortality events.

Although the analytical model developed here required a number of process simplifications, it retains the advantage of producing analytical results that can be applied to large, spatially distributed data sets. It is eminently suitable for coupling with regional-scale climate models. Given the outstanding challenges associated with incorporating ecosystem scale feedbacks into earth system modeling (Lloyd and Farquhar 2008), frameworks of this kind—which make simplifying but justifiable assumptions—provide an approach for synthesizing the complexities of soil, hydrologic, and ecological dynamics into tractable outcomes. Although important theoretical challenges such as linking metrics of plant stress to quantitative predictions of mortality risk remain, stochastic approaches may offer useful avenues for incorporating ecosystem change in large-scale modeling efforts.

Acknowledgments

The authors thank C. Gilligan for his thoughtful discussions regarding plant pathology. S.E.T. acknowledges support from National Science Foundation grant EAR-1013339. I.R.-I. is thankful for the support of NASA under the WaterScapes project NNX08BA43A. I.R.-I. and S.L. acknowledge support from the Andrew W. Mellon Foundation grant "The Dynamics of South African Vegetation."

Literature Cited

Agrios, G. 2005. Plant pathology. Elsevier–Academic Press, San Diego, CA.

Ahimera, N., S. Gisler, D. Morgan, and T. Michailides. 2004. Effects of single drop impactions and natural and simulated rains on the dispersal of *Botryosphaeria doithidea* conidia. Phytopathology 94: 1189–1197.

Allen, C. D., A. K. Macalady, H. Chenchouni, D. Bachelet, N. McDowell, M. Vennetier, T. Kitzberger, et al. 2010. A global overview of drought and heat-induced tree mortality reveals emerging climate change risks for forests. Forest Ecology and Management 259:660–684.

Appell, P. 1925. Sur les fonctions hypergéométriques de plusieurs variables. Gauthier-Villars, Paris

Australian Government Bureau of Meteorology. 2005. Average areal potential evapotranspiration. http://www.bom.gov.au/jsp/ncc/climate_averages/evapotranspiration/index.jsp?maptype=3period=an#maps.0.025degreeresolution.

———. 2007. Average number of days with rainfall greater than 1 mm. http://www.bom.gov.au/jsp/ncc/climate_averages/raindays/index.jsp.0.025degreeresolution.

———. 2009. Average rainfall, spring. http://www.bom.gov.au/jsp/ncc/climate_averages/rainfall/index.jsp.0.025degreeresolution.

Balci, Y., and E. Halmschlager. 2003. Incidence of *Phytophthora* species in oak forests in Austria and their possible involvement in oak decline. Forest Pathology 33:157–174.

Batini, F., and E. Hopkins. 1972. *Phytophthora cinnamomi* rands: a root pathogen of the Jarrah forest. Australian Forestry 36:57–68.

Benjamin, M., and F. Newhook. 1981. Effect of glass microbeads on *Phytophthora* zoospore motility. Transactions of the British Mycological Society 78:43–46.

Benson, D., L. Grand, C. Veria, and T. Gottwald. 2006. Temporal and spatial epidemiology of *Phytophthora* root rot in Fraser fir plantations. Plant Disease 90:1171–1180.

Bergot, M., E. Cloppet, V. Perarnaud, M. Deque, B. Marcais, and M. L. Desprez-Loustau. 2004. Simulation of potential range expansion of oak disease caused by *Phytophthora cinnamomi* under climate change. Global Change Biology 10:1539–1552.

Boland, G., M. Melzer, A. Hopkin, V. Higgins, and A. Nassuth. 2004. Climate change and plant diseases in Ontario. Canadian Journal of Plant Pathology 26:335–350.

Boyer, J. 1995. Biochemical and biophysical aspects of water deficits and the predisposition to disease. Annual Review of Phytopathology 33:251–274.

Brooks, F., and D. Ferrin. 1994. Branch dieback of southern California chaparral vegetation caused by *Botryosphaeria dothidea*. Phytopathology 84:78–83.

Brooks, P., A. Harpold, A. Somor, P. Troch, D. Gochis, B. Ewers, E. Pendall, et al. 2010. Quantifying the effects of mountain pine beetle infestation on water and biogeochemical cycles at multiple spatial and temporal scales. *In* American Geophysical Union Fall Meeting. Abstract B31E-0348.

Brooks, R., and A. Corey. 1964. Hydraulic properties of porous media. Hydrology Paper 3. Colorado State University, Fort Collins.

Bryla, D., and R. Linderman. 2007. Implications of irrigation method and amount of water application on *Phytophthora* and *Pythium* infection and severity of root rot in highbush blueberry. HortScience 42:1463–1467.

Chakraborty, S. 2005. Potential impact of climate change on plant-pathogen interactions. Australasian Plant Pathology 34:443–448.

Chakraborty, S., A. V. Tiedemann, and P. S. Teng. 2000. Climate change: potential impact on plant diseases. Environmental Pollution 108:317–326.

Clapp, R., and G. Hornberger. 1978. Empirical equations for some soil hydraulic properties. Water Resources Research 14:601–604.

Coakley, S., H. Scherm, and S. Chakraborty. 1999. Climate change and plant disease management. Annual Review of Phytopathology 37:399–426.

Commonwealth Science and Industry Research Organization. 2012. ASRIS: Australian Soil Resource Information System. http://www.asris.csiro.au.

Crist, C., and D. Schoeneweiss. 1975. Influence of controlled stresses on susceptibility of European white birch stems to attack by *Botryosphaeria dothidea*. Phytopathology 65:369–373.

Crombie, D., and J. Tippett. 1990. A comparison of water relations, visual symptoms, and changes in stem girth for evaluating impact of *Phytophthora cinnamomi* dieback on *Eucalyptus marginata*. Canadian Journal of Forestry Research 20:233–240.

Davidson, E., and F. Tay. 1995. Predictions of where minimal damage to jarrah roots could result in tree death. New Phytologist 131: 393–401.

Dawson, P., and G. Weste. 1984. Impact of root infection by *Phytophthora cinnamomi* on the water relations of two *Eucalyptus* species that differ in susceptibility. Phytopathology 74:486–490.

Desprez-Loustau, M.-L., B. Marcais, L. M. Nageleisen, D. Piou, and A. Vannini. 2006. Interactive effects of drought and pathogens in forest trees. Annals of Forest Science 63:597–612.

Dickenson, S., and B. Wheeler. 1981. Effects of temperature and water-stress in sycamore on growth of *Cryptostroma corticale*. Transactions of the British Mycological Society 76:181–185.

Environmental Protection and Biodiversity Conservation Act. 1999. Commonwealth of Australia.

Ferrin, D. M., and M. E. Stanghellini. 2006. Effect of water potential on mycelial growth and perithecial production of *Monosporascus cannonballus*. Plant Pathology 55:421–426.

Garrett, K. A., S. P. Dendy, E. E. Frank, M. N. Rouse, and S. E. Travers. 2006. Climate change effects on plant disease: genomes to ecosystems. Annual Review of Phytopathology 44:489–509.

Guardiola-Claramonte, M., P. Troch, D. Breshears, T. Huxman, M. Switanek, M. Durcik, and N. Cobb. 2011. Decreased streamflow in semi-arid basins following drought-induced tree die-off: a counter-intuitive and indirect climate impact on hydrology. Journal of Hydrology 406:225–233.

Harham, A. 2005. *Phytophthora cinnamomi*. Molecular Plant Pathology 6:589–604.

Horsthemke, W., and R. Lefever. 1984. Noise-induced transitions: theory and applications in physics, chemistry and biology. Springer, New York.

Hwang, S. C., and W. Ko. 1978. Biology of chlamydospores, sporangia, and zoospores of *Phytophthora cinnamomi* in soil. Phytopathology 68:726–731.

Ibanez, I., J. Clark, M. Dietze, K. Feeley, M. Hersh, S. LaDeau, A. McBride, N. Welch, and M. Wolosin. 2006. Predicting biodiversity change: outside the climate envelope, beyond the species-area curve. Ecology 87:1896–1906.

Jönsson, U. 2006. A conceptual model for the development of *Phytophthora* disease in *Quercus robur*. New Phytologist 171:55–68.

Judelson, H., and F. Blanco. 2005. The spores of *Phytophthora*: weapons of the plant destroyer. Nature Reviews Microbiology 3:47–58.

Laio, F., A. Porporato, L. Ridolfi, and I. Rodriguez-Iturbe. 2001. Plants in water-controlled ecosystems: active role in hydrologic processes and response to water stress. II. Probabilistic soil moisture dynamics. Advances in Water Resources 24:707–723.

Lloyd, J., and G. Farquhar. 2008. Effects of rising temperatures and [CO_2] on the physiology of tropical forest trees. Philosophical Transactions of the Royal Society B: Biological Sciences 363:1811–1817.

Ma, Z., D. Morgan, and T. Michailides. 2001. Effects of water stress on *Botryosphaeria* blight of pistachio caused by *Botryosphaeria dothidea*. Plant Disease 73:745–749.

MacDonald, J., and J. Duniway. 1978. Influence of the matric and osmotic components of water potential on zoospore discharge in of *Phytophthora*. Ecology and Epidemiology 67:751–757.

Madar, Z., Z. Solel, and M. Kimchi. 1989. Effect of water-stress in cypress on the development of cankers caused by *Diplodia pinea* f.sp. *cupressi* and *Seiridium cardinale*. Plant Disease 73:484–486.

Madar, Z., Z. Solel, and A. Sztejnberg. 1990. The effect of *Diplodia pinea* f.sp. *cupressi* and *Seiridium cardinale* on water flow in cypress branches. Physiological and Molecular Plant Pathology 37:389–398.

Malajczuk, N., and C. Theodorou. 1979. Influence of water potential on growth and cultural characteristics of *Phytophthora cinnamomi*. Transactions of the British Mycological Society 72:15–18.

Maurel, M., C. Robin, X. Capdevielle, D. Loustau, and M. L. Desprez-Loustau. 2001. Effects of variable root damage caused by *Phyto-*

phthora cinnamomi on water relations of chestnut saplings. Annals of Forest Science 58:639–651.

Maxwell, D. L., E. L. Kruger, and G. R. Stanosz. 1997. Effects of water stress on colonization of poplar stems and excised leaf disks by *Septoria musiva*. Phytopathology 87:381–388.

Mayek-Perez, N., J. A. Acosta-Gallegos, and C. Lopez-Castaneda. 2002. Relationship between early vigor of common bean (*Phaseolus vulgaris* l.) and resistance to water stress and to *Macrophomina phaseolina* (tassi) *Goidanich*. Revista Mexicana de Fitopatologia 20: 133–140.

McPartland, J., and D. Schoeneweiss. 1984. Hyphal morphology of *Botryosphaeria dothidea* in vessels of unstresssed and drought stressed stems of *Betula alba*. Phytopathology 74:358–362.

Melloy, P., G. Hollaway, J. Luck, R. Norton, E. Aitken, and S. Chakraborty. 2010. Production and fitness of *Fusarium pseudograminearum* inoculum at elevated carbon dioxide in FACE. Global Change Biology 16:3363–3373.

Muneepeerakul, R., A. Rinaldo, and I. Rodriguez-Iturbe. 2007. Effects of river flow scaling properties on riparian width and vegetation biomass. Water Resources Research 43, doi:10.1029/2007WR006100.

Nesbitt, H., N. Malajczuk, and A. Glenn. 1978. Effect of soil moisture and temperature on the survival of *Phytophthora cinnamomi* rands in soil. Soil Biology and Biochemistry 11:137–140.

Newhook, F., and F. Podger. 1972. The role of *Phytophthora cinnamomi* in Australian and New Zealand forests. Annual Reviews in Phytopathology 10:299–326.

Pacific Northwest Cooperative Agricultural Weather Network. 2012. Corvallis, Oregon, AgriMet station (CRVO). http://usbr.gov/pn/agrimet/.

Pangga, I. B., S. Chakraborty, and D. Yates. 2004. Canopy size and induced resistance in *Stylosanthes scabra* determine anthracnose severity at high CO_2. Phytopathology 94:221–227.

Porporato, A., F. Laio, L. Ridolfi, and I. Rodriguez-Iturbe. 2001. Plants in water-controlled ecosystems: active role in hydrologic processes and response to water stress. III. Vegetation water stress. Advances in Water Resources 24:725–744.

Pusey, P. 1989. Influence of water stress on susceptibility of nonwounded peach bark to *Botryosphaeria dothidea*. Plant Disease 73: 1000–1003.

Rayachhetry, M., G. Blakesee, and T. Miller. 1996. Histopathology of *Botryosphaeria ribis* in *Melaleuca quinquenervia*: pathogen invasion and host response. International Journal of Plant Sciences 157: 219–227.

Rodriguez-Iturbe, I., and A. Porporato. 2004. Ecohydrology of water-controlled ecosystems: soil moisture and plant dynamics. Cambridge University Press, Cambridge.

Rodriguez-Iturbe, I., A. Porporato, L. Ridolfi, V. Isham, and D. R. Cox. 1999. Water balance at a point: the role of climate, soil and vegetation. Proceedings of the Royal Society A 455:3789–3809.

Rolshausen, P., J. Urbez-Torres, S. Rooney-Latham, A. Eskalen, R. Smith, and W. Gubler. 2010. Evaluation of pruning wound susceptibility and protection against fungi associated with grapevine trunk diseases. American Journal of Enology and Viticulture 61: 113–119.

Schober, B., and J. Zadocks. 1999. Water and temperature relations of softrot bacteria: growth and disease development. Annals of Applied Biology 134:59–64.

Schoeneweiss, D. 1986. Water stress predisposition to disease, an overview. Pages 157–174 *in* P. Ayers and L. Boddy, eds. Water, fungi and plants. Cambridge University Press, Cambridge.

Schulte, P., and D. Costa. 2010. Xylem anisotropy and water transport: a model for the double sawcut experiment. Tree Physiology 30:901–913.

Smith, H., G. Kemp, and M. Wingfield. 1994. Canker and dieback of eucalyptus in South Africa caused by *Botryosphaeria dothidea*. Plant Pathology 43:1031–1034.

Sterne, R., G. Zentmyer, and M. Kaufman. 1977*a*. The effect of matric and osmotic potential of soil on phytophthora root rot disease of *Persea indica*. Phytopathology 67:1491–1494.

———. 1977*b*. The effect of matric potential, soil texture and soil amendment on root disease caused by *Phytophthora cinnamomi*. Phytopathology 67:1495–1500.

Suleman, P., A. Al-Musallam, and C. Menezes. 2001. The effect of solute potential and water stress on black scorch caused by *Chalara radicicola* on date palms. Plant Disease 85:80–83.

Tapsoba, H., and J. P. Wilson. 1983. Effects of temperature and light on germination of urediniospores of the pearl millet rust pathogen, *Puccinia substriata* var *indica*. Plant Disease 81:1049–1052.

Thompson, S., P. Alvarez-Loayza, J. Terborgh, and G. Katul. 2010. The effects of plant pathogens on tree recruitment in the western Amazon under a projected future climate: a dynamical systems analysis. Journal of Ecology 98:1434–1446.

Tippett, J., D. Crombie, and T. Hill. 1987. Effect of phloem water relations on the growth of *Phytophthora cinnamomi* in *Eucalyptus marginata*. Phytopathology 77:246–250.

Tippett, J., J. McGrath, and T. Hill. 1989. Site and seasonal effects on susceptibility of *Eucalyptus marginata* to *Phytophthora cinnamomi*. Australian Journal of Botany 37:481–490.

Tregonning, K., and P. Fagg. 1984. Seasonal rainfall and eucalyptus dieback epidemics associated with *Phytophthora cinnamomi* in Gippsland, Victoria. Australian Journal of Forest Research 14:219–234.

Tyree, M. T., and F. W. Ewers. 1991. The hydraulic architectures of trees and other woody plants. New Phytologist 119:345–360.

Vannini, A., and R. Valentini. 1994. Influence of water relations on *Quercus cerris–Hypoxlon mediterraneum* interaction: a model of drought-induced susceptibility to a weakness parasite. Tree Physiology 14:129–139.

Waugh, M. M., D. H. Kim, D. M. Ferrin, and M. E. Stanghellini. 2003. Reproductive potential of *Monosporascus cannonballus*. Plant Disease 87:45–50.

Weste, G., and G. Marks. 1987. The biology of *Phytophthora cinnamomi* in Australasian forests. Annual Review of Phytopathology 25:207–229.

Weste, G., and P. Taylor. 1987. The invasion of native forest by *Phytophthora cinnamomi*. I. Brisbane Ranges, Victoria. Australian Journal of Botany 19:281–294.

Associate Editor: Pejman Rohani
Editor: Mark A. McPeek